

Fig. 2. Illustration of the asymmetric unit in [(CH₃)₃S]₂CuCl₄.

The repulsive S···Cu interaction between two positive species in [(CH₃)₃S]₂Cu₂Cl₆ can be rationalized, based on the structural characteristics observed for the S···Cl interactions in [(CH₃)₃S]₂CuCl₄. A search of the environs of the S atom in [(CH₃)₃S]₂Cu₂Cl₆ reveals numerous short S···Cl interactions, the three shortest of which are correctly positioned so as to define a trigonally distorted octahedral arrangement (Table 5). With two of these S···Cl interactions to Cl atoms on adjacent dimers within a stack, the S atom is located so as to effectively block the sixth octahedral coordination site for the Cu^{II} ion. The third S···Cl interaction is to a Cl atom in an adjacent stack.

The support of NSF (CHE-8408407) and The Boeing Company for establishment of the X-ray diffraction facility is acknowledged. The research was supported in part by NSF grant DMR-88-03382 and PRF Grant 16525-AC3,7.

References

- BOND, M. R. (1990). PhD Thesis, Washington State Univ., USA.
 BOND, M. R. & WILLETT, R. D. (1989). *Inorg. Chem.* **28**, 3267–3269.
 BOND, M. R., WILLETT, R. D. & RUBENACKER, G. (1990). *Inorg. Chem.* **29**, 2713–2720.
 CAMPANA, C. F., SHEPARD, D. F. & LITCHMAN, W. M. (1981). *Inorg. Chem.* **20**, 4039–4044.
 CLAY, R. M., MURRAY-RUST, P. & MURRAY-RUST, J. (1973). *J. Chem. Soc. Dalton. Trans.* pp. 595–599.
 GEISER, U., WILLETT, R. D., LINDBECK, M. & EMERSON, K. (1986). *J. Am. Chem. Soc.* **108**, 1173–1179.
 SHELDRICK, G. M. (1985). *SHELXTL*, version 5.1 Nicolet Analytical Instruments, Madison, WI, USA.
 WEENK, J. & HARWIG, H. A. (1977). *J. Chem. Phys. Solids*, **38**, 1055–1061.
 WEENK, J. & SPEK, A. L. (1976). *Cryst. Struct. Commun.* **5**, 805–809.
 WILLETT, R. D. (1987). *Trans. Met. Chem. (London)*, **12**, 410–413.
 WILLETT, R. D. (1988). *Acta Cryst.* **B44**, 503–508.
 WILLETT, R. D., BOND, M. R., HALJE, W. G., SOONIEUS, O. P. M. & MAASKANT, W. J. A. (1988). *Inorg. Chem.* **27**, 614–620.
 WILLETT, R. D., HALVORSON, K. & PATTERSON, C. (1990). *Acta Cryst.* **C46**, 508–518.

Acta Cryst. (1992). **C48**, 1192–1197

Tetraaquabis(hydrogen maleato)zinc(II) by Neutron Diffraction and Tetraaquabis(hydrogen maleato)nickel(II) by High-Order X-ray Diffraction

BY A. SEQUEIRA AND H. RAJAGOPAL

Neutron Physics Division, Bhabha Atomic Research Centre, CIRUS, Trombay, Bombay 400 085, India

M. P. GUPTA

Department of Physics, University of Ranchi, Ranchi 834 008, India

AND F. VANHOUTEGHEM,* A. T. H. LENSTRA† AND H. J. GEISE

University of Antwerp (UIA), Department of Chemistry, Universiteitsplein 1, B-2610 Wilrijk, Belgium

(Received 26 March 1990; accepted 10 December 1991)

Abstract. Neutron intensities ($\sin\theta/\lambda \leq 0.5 \text{ \AA}^{-1}$) of zinc bis(hydrogen maleate) tetrahydrate,

Zn(C₄H₃O₄)₂·4H₂O, and X-ray intensities ($\sin\theta/\lambda \leq 1.1 \text{ \AA}^{-1}$) of nickel bis(hydrogen maleate) tetrahydrate, Ni(C₄H₃O₄)₂·4H₂O, were collected at room temperature (298 K). Zn salt: $M_r = 367.5$, triclinic, $P\bar{1}$, $a = 7.337(5)$, $b = 9.219(7)$, $c = 5.222(3) \text{ \AA}$, $\alpha =$

* Deceased on 23 January 1991.

† Author to whom correspondence should be addressed.

104.67 (4), $\beta = 93.03$ (9), $\gamma = 108.86$ (9) $^\circ$, $V = 319.6$ \AA^3 , $Z = 1$, $D_m = 1.88$, $D_x = 1.91$ Mg m^{-3} , $\lambda = 1.036$ (1) \AA , $\mu = 0.1675$ mm^{-1} , $R(F) = 0.0245$, $R(F^2) = 0.0329$, $wR(F^2) = 0.0529$ for 696 reflections. Ni salt: $M_r = 360.9$, triclinic, $P\bar{1}$, $a = 7.309$ (3), $b = 9.134$ (2), $c = 5.170$ (2) \AA , $\alpha = 104.65$ (3), $\beta = 92.88$ (3), $\gamma = 108.40$ (2) $^\circ$, $V = 313.6$ (4) \AA^3 , $Z = 1$, $D_m = 1.89$, $D_x = 1.91$ Mg m^{-3} , $\lambda(\text{Mo K}\alpha) = 0.71069$ \AA , $\mu = 1.61$ mm^{-1} , $F(000) = 186$, $R = 0.033$ and $wR = 0.048$ for 7284 reflections and 118 parameters (full-angle refinement). $R = 0.047$ and $wR = 0.051$ for 2677 reflections and 97 parameters (high-order refinement, $0.9 \leq \sin\theta/\lambda \leq 1.1$ \AA^{-1}). The neutron model of the Zn salt and the high-order model of the Ni salt show great similarity. The hydrogen maleate geometry proved to be independent of the nature of the counter ion; bond lengths in the heavy-atom skeleton differ by less than 0.004 \AA and valence angles by less than 0.5 $^\circ$. Differences between Zn—O and the corresponding Ni—O distances are (much) larger, partly reflecting the difference in effective ionic radii of Zn^{II} and Ni^{II} . Hydrogen bonding reduces the symmetry of the metal coordination from O_h to C_i and that of the hydrogen maleate ion from C_{2v} to C_1 . The hydrogen-bonding scheme is accurately determined. A three-centre bifurcated donor hydrogen bond is observed. A very short [2.410 (4) \AA] asymmetric intramolecular hydrogen bond is found (O—H = 1.097 \AA , O \cdots H = 1.316 \AA). The difference Fourier map, calculated from the high-order Ni-salt model in combination with the full-angle data, is close to a deformation density.

Introduction. The structure of the hydrogen maleate ion (henceforth abbreviated as HM) has been the subject of great interest. Both X-ray and neutron diffraction studies have been made (Olovsson, Olovsson & Lehmann, 1984; Gupta, Geise & Lenstra, 1984; Gupta, Van Alsenoy & Lenstra, 1984; Vanhouteghem, Lenstra & Schweiss, 1987) to investigate the influence of counter ions and packing on the geometry and internal hydrogen bond. The isostructural series tetraaquabis(hydrogen maleate)metal(II), $M(\text{C}_4\text{H}_3\text{O}_4)_2 \cdot 4\text{H}_2\text{O}$, with $M = \text{Zn, Mn, Fe, Co}$ and Ni , has been studied in the past by one of us (MPG) and co-workers, but, except for $\text{Ni}(\text{C}_4\text{H}_3\text{O}_4)_2 \cdot 4\text{H}_2\text{O}$ (Gupta, Geise & Lenstra, 1984), no accurate X-ray results have been published. Furthermore, H atoms have not been very precisely located and electronic features were not studied at all. The present work therefore reports on two new investigations. One concerns a new neutron diffraction analysis of the Zn salt, more accurate than the previous one by Antsyshkina, Dikareva, Porai-Koshits, Fykin, Didarev & Guseinov (1982). The other uses full-angle and high-order X-ray data of the Ni salt to arrive at *quasi*-neutron coordinates of non-H atoms.

The aim is twofold. First, to investigate the geometry as a function of the counter ion with a constant hydrogen-bonding scheme and, second, to probe qualitatively the electronic features of the HM ion by comparing the experimental difference Fourier map with the calculated quantum-mechanical deformation density.

Experimental. Crystals of zinc and nickel hydrogen maleate were prepared by slow evaporation of the aqueous solution. Crystals suitable for X-ray studies were easily obtained. Large crystals, as required in a neutron analysis, could only be made for the Zn salt. The larger specimens of the Ni compound were never single crystals. D_m of compounds by flotation.

Neutron data were recorded at room temperature (298 K) using the TDC-312 computer-controlled four-circle diffractometer (Sequeira *et al.*, 1978) at the CIRUS reactor at Trombay, India. The crystal ($3.2 \times 3.0 \times 9.0$ mm) was mounted with its a axis (*i.e.* the long edge) along the φ axis of the diffractometer. The cell parameters and the crystal orientation were refined from the peak positions of over 50 random strong reflections. Intensities of 696 independent reflections with $\sin\theta/\lambda \leq 0.50$ \AA^{-1} [$\lambda = 1.036$ (1) \AA] were recorded in the $\theta/2\theta$ step-scanning mode. Two standard reflections (001 and 020) were recorded at intervals of every 20 reflections to monitor the stability of the crystal and the measuring apparatus. Intensity fluctuations of these standards were within 2% of their mean values during the entire experiment. The integrated intensities were reduced to F_o^2 values by applying standard Lorentz and absorption corrections [not included in the previous work (Antsyshkina *et al.*, 1982)]. With a calculated linear absorption coefficient $\mu = 0.1675$ mm^{-1} , transmission factors were in the range 0.95 to 0.96.

The positions of the H atoms were located in a 3D Fourier map computed using the observed neutron F_o values and the phases calculated on the basis of X-ray non-H-atom positions (Gupta & Ram, 1977). The structural parameters, along with a scale factor and an extinction parameter, were refined by full-matrix least squares on F^2 using the program *TRXFLS* (Rajagopal & Sequeira, 1977, unpublished), a modified version of *ORFLS* (Busing, Martin & Levy, 1962). Weights were given by $w = [\sigma^2(F_o^2) + (0.035F_o^2)^2]^{-1}$. The neutron scattering lengths used were: $b_{\text{H}} = -3.78$, $b_{\text{C}} = 6.65$, $b_{\text{O}} = 5.80$ and $b_{\text{Zn}} = 5.68$ fm (*International Tables for X-ray Crystallography*, 1974, Vol. IV). All atoms were refined anisotropically. An isotropic extinction parameter (Zachariasen, 1967) was included in the refinement, which converged to $R(F) = 0.0245$, $R(F^2) = 0.0329$ and $wR(F^2) = 0.0529$ based on 696 reflections. The final value of the error of fit function $[w\Delta^2/(n-m)]^{1/2} = 1.11$, and $(\Delta/\sigma)_{\text{max}} = 0.1$. The

highest peak in the final difference Fourier map was 4% of the scattering length of the C-atom densities. The refined atomic coordinates* are given in Table 1 and the numbering scheme of atoms in Fig. 1. Compared to the previous analysis (Antsyshkina *et al.*, 1982) the structural features are essentially equal, but the present e.s.d.'s are about a factor of two lower.

Some differences between the neutron geometry of the Zn salt and that of the standard X-ray Ni salt (Gupta, Geise & Lenstra, 1984) were found to be outside the statistical error limits. Therefore a new set of X-ray data of the Ni salt was collected at room temperature on the Enraf-Nonius CAD-4 diffractometer at Antwerpen using graphite-monochromated Mo radiation. The crystal (size 0.1 × 0.1 × 0.15 mm) showed a near isotropic mosaic spread. The distribution could be described by a Lorentzian function with a half width of 0.18 (1)°. The proper alignment of the crystal was proved by the constancy of the signal during azimuth scans. To reduce possible errors caused by multiple scattering all intensities up to $\sin\theta/\lambda = 0.6 \text{ \AA}^{-1}$ were measured at three different ψ angles (-5, 0, 5°). Scan times with a maximum of 150 s were adapted to attain 1% accuracy in terms of counting statistics. The internal agreement factors for the three sets were $R_i(F^2) = 0.03, 0.02$ and 0.03 , respectively. The low-order data were later combined, after having removed outliers with χ^2 statistics. Reflections from $\sin\theta/\lambda = 0.6$ to 1.1 \AA^{-1} were measured once, either with an error margin of 1%, or with a maximum scan time of 6 min per observation. Cell parameters determined from 25 high-order reflections. Three intensity control reflections (510, $\bar{2}71$, 013), measured every 2 h, showed no significant drift during the entire experiment. In this way 10 054 intensities were obtained of which 7284 were considered observed [$I \geq 3\sigma(I)$] in the ranges $-17 \leq h \leq 17$, $-23 \leq k \leq 23$, $0 \leq l \leq 12$. No absorption correction was made ($\mu = 1.61 \text{ mm}^{-1}$). Each reflection was given an individual weight based on counting statistics. To check the accuracy of the full-angle (FA) data set ($0 \leq \sin\theta/\lambda \leq 1.1 \text{ \AA}^{-1}$) a full-matrix refinement on F was performed starting from the parameters of Gupta, Geise & Lenstra (1984), using anisotropic thermal parameters for the non-H atoms and $B_{\text{iso}} = 2.5 \text{ \AA}^2$ for H atoms. Convergence was reached at $R = 0.033$, $wR = 0.048$, $S = 1.8$, $(\Delta/\sigma)_{\text{max}} = 0.1$ for 118 variables and the highest peak in the final difference Fourier $|\rho| = 1.35 \text{ e \AA}^{-3}$. Scattering factors from *International Tables for X-ray Crystallography* (1974, Vol. IV).

Table 1. *Positional parameters in fractions of the cell edges, with e.s.d.'s in parentheses, and isotropic thermal parameters*

Equivalent isotropic thermal parameters (\AA^2) for non-H atoms were calculated according to Lipson & Cochran (1968) [$B_{\text{iso}} = 8\pi^2 (U_{11}^2 + U_{22}^2 + U_{33}^2)^{1/3}$], assuming equal volume of the 50% probability region. All anisotropic thermal parameters were physically acceptable. H(j, x) with $j = 1, 2$ is attached to atom x .

	x	y	z	B_{iso}
Zn salt (neutron data)				
Zn	0.0000	0.0000	0.0000	1.87
O(W1)	0.1342 (4)	-0.0979 (3)	-0.3171 (5)	2.18
O(W2)	0.2593 (4)	0.0780 (4)	0.2496 (4)	2.60
O(1)	-0.0598 (3)	-0.2056 (2)	0.1436 (3)	2.87
O(2)	-0.2707 (3)	-0.3824 (2)	-0.2004 (4)	2.75
O(3)	-0.4538 (3)	-0.6654 (3)	-0.3410 (4)	1.72
O(4)	-0.4740 (3)	-0.8743 (2)	-0.1965 (4)	2.08
C(1)	-0.1706 (2)	-0.3450 (2)	0.0256 (3)	2.23
C(2)	-0.1778 (2)	-0.4676 (2)	0.1673 (3)	2.01
C(3)	-0.2732 (2)	-0.6263 (2)	0.0855 (3)	2.11
C(4)	-0.4072 (2)	-0.7293 (2)	-0.1652 (3)	2.25
H(C2)	-0.0910 (6)	-0.4177 (4)	0.3608 (9)	4.02
H(C3)	-0.2553 (6)	-0.6947 (4)	0.2188 (8)	4.24
H(O3)	-0.3752 (6)	-0.5360 (6)	-0.2851 (7)	4.13
H(1,OW1)	0.0668 (6)	-0.1286 (4)	-0.4968 (9)	3.52
H(2,OW1)	0.2600 (8)	-0.0244 (5)	-0.3148 (7)	3.83
H(1,OW2)	0.3321 (7)	0.1852 (7)	0.3292 (9)	4.55
H(2,OW2)	0.3461 (6)	0.0190 (6)	0.2209 (7)	3.78
Ni salt (high-order X-ray data, $0.9 \leq \sin\theta/\lambda \leq 1.1 \text{ \AA}^{-1}$)				
Ni	0.0000	0.0000	0.0000	1.22
O(W1)	0.1330 (2)	-0.0974 (1)	-0.3142 (2)	1.72
O(W2)	0.2523 (2)	0.0755 (1)	0.2540 (2)	1.74
O(1)	-0.0595 (2)	-0.2018 (1)	0.1402 (2)	1.62
O(2)	-0.2740 (3)	-0.3796 (1)	-0.2026 (2)	2.14
O(3)	-0.4579 (3)	-0.6657 (1)	-0.3401 (3)	2.34
O(4)	-0.4763 (2)	-0.8743 (1)	-0.1888 (3)	2.22
C(1)	-0.1708 (2)	-0.3420 (1)	0.0228 (2)	1.45
C(2)	-0.1756 (2)	-0.4655 (1)	0.1657 (2)	1.74
C(3)	-0.2714 (2)	-0.6249 (1)	0.0874 (3)	1.76
C(4)	-0.4082 (2)	-0.7291 (1)	-0.1621 (3)	1.67

The full-angle model is not given because it does not add information beyond that previously published (Gupta, Geise & Lenstra, 1984). In order to obtain the *quasi*-neutron coordinates needed for a correct comparison of the two salts a series of ten high-order (HO) refinements was performed on data sets with $\sin\theta/\lambda$ thresholds varying from 0.1 to 1.0 \AA^{-1} in steps of 0.1 \AA^{-1} . It was found that a complete model, including H-atom positions, was still refinable up to the data set $0.7 \leq \sin\theta/\lambda \leq 1.1 \text{ \AA}^{-1}$. From this we estimate that electronic features of 0.02 electron can still be recognized and thus the FA difference Fourier contains electronic information.

However, at the $\sin\theta/\lambda = 0.7 \text{ \AA}^{-1}$ threshold the distances between non-H atoms had not yet converged. Therefore, in the further high-order (HO) refinements we initially fixed the H atoms at their full-angle parameters and later at the neutron parameters of the Zn salt (see below). With this strategy convergence of heavy-atom distances was reached with the set $0.9 \leq \sin\theta/\lambda \leq 1.1 \text{ \AA}^{-1}$. The statistics for the refinement of the set are $R = 0.047$, $wR = 0.051$, $S = 1.2$, $(\Delta/\sigma)_{\text{max}} = 0.1$ for 97 variables and 2677 reflections. Table 1 gives the coordinates of this HO model.

* Lists of structure factors and anisotropic thermal parameters of the Zn and Ni salts have been deposited with the British Library Document Supply Centre as Supplementary Publication No. SUP 54826 (24 pp.). Copies may be obtained through The Technical Editor, International Union of Crystallography, 5 Abbey Square, Chester CH1 2HU, England.

Discussion. Table 2 presents the molecular geometry of the neutron structure of the Zn salt and the HO model (heavy-atom skeleton) of the Ni salt. One notes that the differences in the geometry of the HM ion in the two salts are less than 0.004 Å for bond distances and less than 0.5° for valence angles, *i.e.* less than two times their estimated standard deviations. We conclude that the HO model for room-temperature data has produced nuclear positions for the non-H atoms and that the HM geometry is independent of the nature of the counter ion if the hydrogen-bonding scheme is constant.

Concerning the metal coordination the following remarks seem in order. First, much larger differences are found between the two salts than in the HM ion, but the observed difference of 0.041 Å between the *average* Zn—O (2.105 Å) and Ni—O (2.064 Å) distances practically coincides with the difference of 0.05 Å between the effective ionic radii of Zn^{II} and Ni^{II} in the same coordination (Shannon & Prewitt, 1969). Second, the large spread in the individual distances $\{s = [\frac{1}{2}\sum(\text{ZnO} - \text{NiO})^2]^{\frac{1}{2}} = 0.016 \text{ \AA}\}$ suggests the occurrence of one or more effects beyond the ionic hard spheres model. Possible causes include differences in covalent metal–oxygen bond orders (charge-transfer effect) and differences in apparent bond shrinkages arising from differences in torsional/librational force constants (artefacts owing to modelling the temperature-dependent motion of atoms in a solid by a rectilinear β tensor). The occurrence of these effects in magnesium bis(hydrogen maleate) hexahydrate was demonstrated in a recent study (Vanhouteghem, Helmholdt, Lenstra, Peeters & Van Alsenoy, 1992). Shrinkage causes

uncertainties in positional coordinates and thus impairs the determination of deformation density $\Delta\rho$ (XN) (see below). Third, the metal coordination can only to a first approximation be described as a distorted octahedron. The true symmetry is C_i , because of the chemical difference between the coordinating O atoms and the positioning of the water H atoms. This distortion is linked to the formation of hydrogen bonds to neighbouring acceptors.

Table 3 presents the hydrogen-bonding scheme based on the H-atom positions of the Zn salt, as determined by neutron diffraction. The existence of a three-centre bifurcated hydrogen bond, previously reported by Gupta, Geise & Lenstra (1984) for Ni^{II}-(C₄H₃O₄)₂·4H₂O, is confirmed. The geometrical details, more accurate than before, are shown in Table 3. The neutron analysis yielded the following details for the short intramolecular hydrogen bridge in the HM ion: O(2)⋯O(3) = 2.410 (4), O(3)—H = 1.097 (7), O(3)H⋯O(2) = 1.316 (5) Å, asymmetry Δ (OH⋯O) = 1.316–1.097 = 0.219 Å, O(3)—H⋯O(2) = 174.7 (4)°. It fits reasonably well in the correlation between bonded O(3)—H and non-bonded O(3)H⋯O(2) distances in hydrogen maleates proposed by Olovsson, Olovsson & Lehmann (1984). Since there is no evidence for disorder in this intramolecular hydrogen bond, packing forces must have a decisive influence on the shape of the potential governing the position of H between O(3) and O(2). Further, since O(3) is clearly the donor and O(2) the acceptor, the HM ion has neither approximate C_2 , nor C_s symmetry. Also it is confirmed that the two carboxyl groups are rotated out of the plane of the four C atoms in a disrotatory rather than a con-

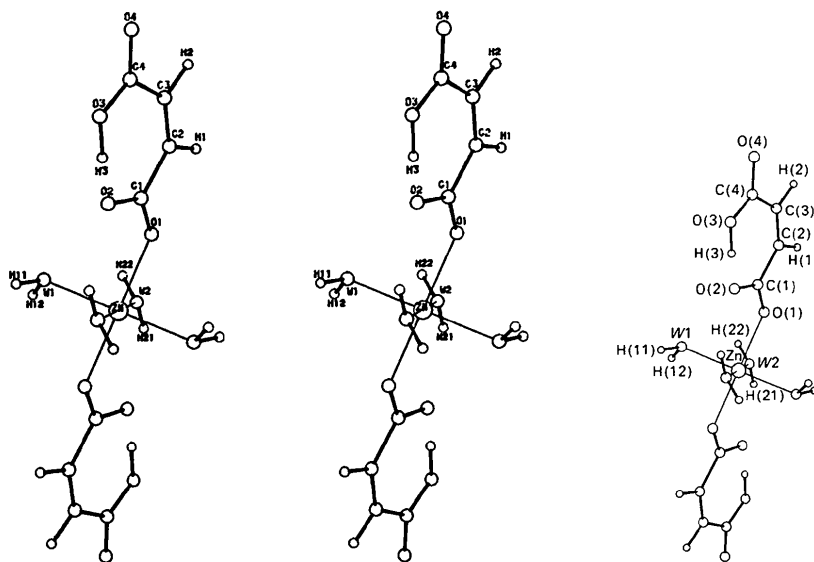


Fig. 1. PLUTO (Motherwell & Clegg, 1978) drawing showing atomic numbering scheme of the Zn compound next to a stereoview.

Table 2. Metal coordination and geometry of the HM ions (Å, °)

Metal at an inversion centre; e.s.d.'s in parentheses.		
	Zn-HM Neutron data	Ni-HM High-order X-ray data
Metal coordination		
M—O(1)	2.136 (2)	2.078 (1)
M—O(W1)	2.125 (2)	2.089 (1)
M—O(W2)	2.053 (2)	2.025 (1)
H(1,OW1)—O(W1)	0.965 (7)	
H(2,OW1)—O(W1)	0.950 (8)	
H(1,OW2)—O(W2)	0.929 (8)	
H(2,OW2)—O(W2)	0.957 (9)	
O(1)—M—O(W1)	92.38 (7)	92.45 (8)
O(1)—M—O(W2)	96.44 (9)	96.73 (10)
O(W1)—M—O(W2)	91.18 (11)	90.25 (9)
H(1,OW1)—O(W1)—H(2,OW1)	106.40 (38)	
H(1,OW2)—O(W2)—H(2,OW2)	108.72 (42)	
H(1,OW1)—O(W1)—M	117.30 (37)	
H(2,OW1)—O(W1)—M	110.24 (31)	
H(1,OW2)—O(W2)—M	123.65 (49)	
H(2,OW2)—O(W2)—M	120.23 (27)	
C(1)—O(1)—M	127.24 (14)	
H(1,OW1)—O(W1)—M—O(W2)	-165.6 (4)	
H(1,OW1)—O(W1)—M—O(1)	110.9 (3)	
H(2,OW1)—O(W1)—M—O(W2)	-43.7 (4)	
H(2,OW1)—O(W1)—M—O(1)	-127.2 (4)	
H(1,OW2)—O(W2)—M—O(W1)	115.3 (4)	
H(1,OW2)—O(W2)—M—O(1)	-152.2 (4)	
H(2,OW2)—O(W2)—M—O(W1)	-31.1 (4)	
H(2,OW2)—O(W2)—M—O(1)	61.4 (4)	
C(1)—O(1)—M—O(W1)	-64.8 (2)	-65.0 (3)
C(1)—O(1)—M—O(W2)	-153.3 (2)	-154.6 (3)
HM geometry		
O(1)—C(1)	1.250 (2)	1.254 (1)
O(2)—C(1)	1.261 (2)	1.262 (1)
O(3)—C(4)	1.295 (3)	1.298 (1)
O(4)—C(4)	1.229 (2)	1.229 (1)
C(1)—C(2)	1.489 (2)	1.491 (1)
C(2)—C(3)	1.342 (2)	1.343 (1)
C(3)—C(4)	1.488 (2)	1.491 (1)
C(2)—H(C2)	1.070 (5)	
C(3)—H(C3)	1.080 (5)	
O(3)—H(O3)	1.097 (7)	
O(3)—O(2)	2.410 (4)	2.429 (2)
O(1)—H(O3)	1.317 (5)	
O(1)—C(1)—O(2)	123.03 (16)	123.3 (1)
O(1)—C(1)—C(2)	115.98 (14)	116.0 (1)
O(2)—C(1)—C(2)	120.99 (15)	120.8 (1)
C(1)—C(2)—C(3)	129.51 (16)	130.0 (1)
C(2)—C(3)—C(4)	130.55 (16)	130.6 (1)
O(3)—C(4)—O(4)	121.71 (18)	121.6 (2)
O(3)—C(4)—C(3)	120.03 (16)	120.2 (1)
O(4)—C(4)—C(3)	118.25 (16)	118.2 (2)
C(1)—C(2)—H(C2)	112.71 (22)	
C(3)—C(2)—H(C2)	117.77 (24)	
C(2)—C(3)—H(C3)	117.61 (24)	
C(4)—C(3)—H(C3)	111.83 (23)	
C(4)—O(3)—H(O3)	111.77 (26)	
O(3)—H(O3)···O(1)	174.65 (38)	
O(1)—C(1)—C(2)—C(3)	-175.9 (2)	-176.4 (4)
O(2)—C(1)—C(2)—C(3)	3.8 (3)	3.5 (7)
C(1)—C(2)—C(3)—C(4)	-2.7 (3)	-2.2 (7)
C(2)—C(3)—C(4)—O(3)	-3.0 (3)	-3.2 (6)
C(2)—C(3)—C(4)—O(4)	178.4 (2)	179.1 (4)

rotatory fashion. The C(1)O(1)O(2) group is rotated over 2.6 (Zn) and 2.9° (Ni) and the C(4)O(3)O(4) group over 4.0 (Zn) and 3.5° (Ni).

As stated before, the full-angle difference Fourier map must contain features above a mere noise level. The counting statistical uncertainties in the intensity measurements lead to the estimate $\sigma(\rho) = 0.015 \text{ e } \text{Å}^{-3}$, in agreement with the minimum recog-

Table 3. Hydrogen-bonding scheme (Å, °)

D	A	A at	D—H	H···A	D···A	D—H···A
O(W1)—H(1,OW1)	O(1)	x, y, z-1	0.965 (7)	1.899 (5)	2.861 (3)	174.9 (3)
O(W1)—H(2,OW1)	O(4)	x+1, y+1, z	0.950 (8)	1.949 (6)	2.869 (3)	162.4 (4)
O(W2)—H(2,OW2)	O(4)	-x, -y-1, -z	0.957 (9)	1.848 (7)	2.789 (4)	167.4 (4)
O(W2)—H(1,OW2)	O(2)	-x, -y, -z	0.929 (8)	2.253 (5)	2.792 (3)	122.2 (4)
O(3)—H(3)	O(3)	x+1, y+1, z+1	2.108 (6)	2.888 (3)	140.8 (4)	
	O(2)	x, y, z	1.097 (7)	1.316 (5)	2.410 (4)	174.7 (4)

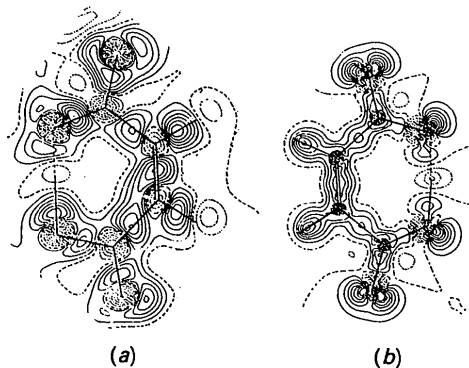


Fig. 2. (a) Difference Fourier density in the plane of the C-atom skeleton of the HM ion (see text) using all data up to $\sin\theta/\lambda = 1.1 \text{ Å}^{-1}$. Full lines represent positive contours, the intense dashed line is the zero contour, less intense dashed lines represent the negative contours. Highest positive maximum is 0.4, lowest negative minimum is $-0.4 \text{ e } \text{Å}^{-3}$. Lines are equally spaced (spacing $0.07 \text{ e } \text{Å}^{-3}$) between zero and the extreme values. (b) Static deformation density obtained by *ab-initio* methods.

nizable $\rho = 0.02 \text{ e } \text{Å}^{-3}$ (see above). In contrast the set of ΔF values after least-squares optimization leads to $\sigma(\rho) = 0.2 \text{ e } \text{Å}^{-3}$. If the order-of-magnitude difference is connected with the neglect of bonding effects in the structure model itself then a difference Fourier map based on the HO model in combination with the full-angle data should resemble a deformation density. The experimental difference Fourier map in the HM plane is depicted in Fig. 2(a) and may be compared with the theoretical static deformation map given in Fig. 2(b). The latter is enumerated using the program TEXAS (Pulay, 1979) and ATOMSCF (van Duynveldt, 1971). The HM geometry on the 4-21G *ab-initio* level with complete geometry relaxation was taken from Vanhouteghem, Lenstra & Schweiss (1987). We conclude that the difference Fourier map is indeed close to a deformation density and that $\sigma(\rho) = 0.02 \text{ e } \text{Å}^{-3}$ is a faithful estimate of its resolution. Furthermore, the non-random distribution of 'least-squares noise' [Fig. 2(a)] agrees with other qualitative deformation density distributions of the HM moiety (Hsu & Schlemper, 1980).

The close parallel between experimental and theoretical maps, despite the use of room-temperature data, is undoubtedly promoted by the small values of the atomic temperature parameters. Nevertheless, a

quantitative transformation of the experimental difference Fourier map into a dynamic deformation density map is precluded, because at room temperature thermal movements give rise to uncertainties in bond lengths of about 0.01 Å, as demonstrated in the corresponding Mg salt (Gupta, Geise & Lenstra, 1984; Vanhouteghem, Lenstra & Schweiss, 1987). Such bond-length uncertainties cause uncertainties in atomic positions too large for a meaningful multipole analysis.

References

- ANTSYSKHINA, A. S., DIKAREVA, L. M., PORAI-KOSHITS, M. A., FYKIN, L. E., DIDAREV, V. YU. & GUSEINOV, M. G. (1982). *Koord. Khim.* **8**, 1256–1260.
- BUSING, W. R., MARTIN, K. O. & LEVY, H. A. (1962). *ORFLS*. Report ORNL-TM-305. Oak Ridge National Laboratory, Tennessee, USA.
- DUYNENVELDT, F. B. VAN (1971). In *Gaussian Basis Sets for the Atoms H–Ne for Use in Molecular Calculations*. IBM Research Report RJ945.
- GUPTA, M. P., GEISE, H. J. & LENSTRA, A. T. H. (1984). *Acta Cryst.* **C40**, 1152–1154.
- GUPTA, M. P. & RAM, P. (1977). National Conference on Crystallography, Madras, India, p. 12.
- GUPTA, M. P., VAN ALSENOY, C. & LENSTRA, A. T. H. (1984). *Acta Cryst.* **C40**, 1526–1529.
- HSU, B. & SCHLEMPER, E. O. (1980). *Acta Cryst.* **B36**, 3017–3023.
- LIPSON, H. & COCHRAN, W. (1968). *The Determination of Crystal Structures*, pp. 307ff. London: Bell.
- MOTHERWELL, W. D. S. & CLEGG, W. (1978). *PLUTO*. Program for plotting molecular and crystal structures. Univ. of Cambridge, England.
- OLOVSSON, G., OLOVSSON, I. & LEHMANN, M. S. (1984). *Acta Cryst.* **C40**, 1521–1526.
- PULAY, P. (1979). *Theor. Chim. Acta*, **50**, 299–312.
- SEQUEIRA, A., MOMIN, S. N., RAJAGOPAL, H., SONI, J. N., CHIDAMBARAM, R., DILIP KUMAR, RAO, R. A. & GOPU, V. M. (1978). *Pramana*, **10**, 289–302.
- SHANNON, R. D. & PREWITT, C. T. (1969). *Acta Cryst.* **B25**, 925–946.
- VANHOUTEGHEM, F., HELMHOLDT, R. B., LENSTRA, A. T. H., PEETERS, A. & VAN ALSENOY, C. (1992). To be submitted.
- VANHOUTEGHEM, F., LENSTRA, A. T. H. & SCHWEISS, P. (1987). *Acta Cryst.* **B43**, 523–528.
- ZACHARIASEN, W. H. (1967). *Acta Cryst.* **23**, 558–564.

Acta Cryst. (1992). **C48**, 1197–1199

Structure of (2-Ammonioethyl methyl sulfoxide)trichloroplatinum(II)

BY EDWINA C. H. LING, GREGORY W. ALLEN AND TREVOR W. HAMBLEY

Department of Inorganic Chemistry, University of Sydney, Sydney, NSW 2006, Australia

(Received 24 September 1991; accepted 25 November 1991)

Abstract. [Pt{CH₃(SO)CH₂CH₂NH₃}Cl₃], $M_r = 409.61$, monoclinic, $P2_1/n$, $a = 7.063$ (2), $b = 13.000$ (2), $c = 10.628$ (3) Å, $\beta = 96.86$ (1)°, $V = 969.0$ (4) Å³, $D_x = 2.81$ g cm⁻³, $Z = 4$, $Mo K\alpha$, $\lambda = 0.71069$ Å, $\mu = 161.8$ cm⁻¹, $F(000) = 752$, $T = 294$ K, final $R = 0.029$ for 2218 reflections. The amine-sulfoxide ligand is coordinated to the Pt centre *via* the S donor atom only, the Pt–S bond length being 2.205 (1) Å. The Pt–Cl bond lengths range from 2.286 (2) to 2.325 (2) Å. The geometry about Pt is approximately square planar.

Introduction. On the basis of molecular mechanics studies, it has been proposed that destabilizing interactions prevent the chemotherapeutic drug cisplatin {[Pt(NH₃)Cl₂]} from binding intrastrand to GpA sequences of DNA (Hambley, 1991). We have designed and synthesized a series of platinum sulfoxide complexes including [Pt{CH₃(SO)CH₂CH₂NH₂}Cl₂], which avoid these unfavourable interactions and thereby target such DNA sequences (Ling, Allen & Hambley, 1991). Unlike closely

related compounds, [Pt{CH₃(SO)CH₂CH₂NH₂}Cl₂] proved difficult to synthesize as the sulfoxide ligand readily coordinated to the Pt centre in a monodentate fashion *via* the S donor atom. A mixture of both [Pt{CH₃(SO)CH₂CH₂NH₂}Cl₂] and [Pt{CH₃(SO)CH₂CH₂NH₃}Cl₃] was usually produced upon reaction of the protonated or basic forms of the CH₃(SO)CH₂CH₂NH₂ ligand with K₂[PtCl₄], acidic conditions (pH ≤ 3) favouring formation of the trichloro complex. We have structurally characterized both of these complexes and herein report the results for the latter.

Experimental. Solutions of K₂[PtCl₄] and CH₃-(SO)CH₂CH₂NH₂.HCl were combined, yielding orange crystals of the title compound and pale yellow crystals of [Pt{CH₃(SO)CH₂CH₂NH₂}Cl₂] in a ratio of *ca* 4:1. A crystal was mounted on a glass fibre with epoxy resin and data collected using an Enraf-Nonius CAD-4 diffractometer, graphite-monochromated radiation. 25 independent reflections with $20 \leq 2\theta \leq 30^\circ$ were used for least-squares